Lampyrid 2023: Volume 13, 112–116
ISSN: 2041-4900
https://lampyridjournal.com

Fabrication and Characterization of Niobium Alloys Treated by Vacuum Arc Remelting Technique: Hybrid Approach for Orthopedic Applications

B. Vinod[1*], K. Sai Sujith[2], A. Suresh[3], P. Venkataramana[4]
[1, 2,3,4] Department of Mechanical Engineering,
Siddharth Institute of Engineering & Technology, Puttur, Andhra Pradesh, India

Abstract

This research showed the wear and mechanical behaviour of two new Ti-Nb-based alloys for biomedical implants. Vacuum arc remelting is used to create two types of Ti-Nb alloys with different elemental percentages of niobium: Ti-35Nb-7Zr-5Ta-0.35O and Ti-24Nb-4Zr-8Sn. The alloys were treated with heat at 2000^{o}C for 6 hours in an argon atmosphere. Field emission scanning electron microscopy was used to determine the microstructure and confirm the phase. Vickers microhardness testing was used to determine the alloys' hardness. A pin-on-disc wear testing equipment is used to conduct in-vitro tests to determine the samples' resistance to wear. Comparisons with Ti-24Nb-4Zr-8Sn showed that the alloys' coefficient of friction was improved by order of magnitude.
Keywords: Niobium alloys, Tribology, Orthopedic applications, Morphology, Mechanical properties

INTRODUCTION

The most important characteristics of a biomedical application, such as a knee implant, are strong biocompatibility, good corrosion resistance, high wear resistance, and a low modulus of elasticity. Conventional implant materials like stainless steel and cobalt-chromium alloys have a high elastic modulus (200–220 GPa) [1] compared to the cortical bone (30 GPa), which can cause allergic reactions, inflammations, and blood clotting and even necessitate revision surgery in some cases [2]. On the other hand, titanium alloys have recently gained attention as a promising implant material for knee implants because of their excellent corrosion resistance, good biocompatibility, and decreased elastic modulus [3]. Although Ti-based biomedical implants have shown promising results, the low wear resistance of the Ti alloys continues to be a vital issue. Wear debris is created when two surfaces, the implant and the bone, or two joint elements, are in motion relative to one another [4]. As the body accumulates worn debris, inflammation, infection, allergy, and pain are triggered in the area. Implant loosening and eventual fracture may also result from wear. For this reason, improving the wear resistance of Ti-based biomedical implants is crucial to their widespread use. When there is a significant disparity between the implant and the human bone in moduli, a phenomenon known as stress shielding [5] occurs. The mechanical stress occurring on the implant is not transferred effectively to the neighbouring bone. As a result, the implant becomes loose and eventually fails. Relative motion between two surfaces, such as an implant and bone or two joint elements, causes wear and affects or consumes the substance [6]. The present investigation utilised three custom-made Ti-Nb alloys with slightly different elemental breakdowns. The main aim of the work is:

- The effect of stress shielding can be lessened by lowering the elasticity of the above Ti-Nb alloys.
- These study objectives are to conduct extensive wear testing at three distinct loads to investigate the alloys' in-vitro wear behaviour and report the results of this research.
- Mechanical testing to investigate how the alloys react to each other.

2. EXPERIMENTAL STUDIES

2.1 Preparation of the alloys

The metals in the crucible are melted by striking an electric arc between a non-consumable Tungsten electrode and the metals, resulting in an alloy. This process, known as vacuum arc melting, occurs in an argon atmosphere. The molten alloy is the result of the melting of the metals in the crucible caused by the generated heat. Ensure evenly distributed alloy melting is repeated. To prevent the alloys from oxidising during melting, the chamber is evacuated by purging it with argon gas. Alloys can be melted at temperatures of 2000^{o}C. As part of the current study, two Ti-Nb-based alloys, Ti-35Nb-7Zr-5Ta-0.35O and Ti-24Nb-4Zr-8Sn, were produced using vacuum arc melting [7]. The alloy metal pieces are first placed in a crucible. The chamber was emptied using Ar gas before the melting process began to keep the alloys pure. For this melting procedure, a tungsten electrode not consumed by the operation was used to strike an electric arc into the metal fragments in the crucible. After cooling to normal temperature, the molten substance solidified.

2.2 Heat treatment

Typically, heat treatments are applied to alloys to achieve the desired microstructures, which affect the alloys' mechanical characteristics and remove the stresses introduced during production. Alloys undergo various heat treatments, including annealing, case hardening, precipitation strengthening, tempering, normalizing, and quenching. Alloys' strength and other mechanical qualities are optimized by applying controlled heating and cooling by their phase diagrams. In this study, three manufactured alloys were subjected to heat treatment in a tube furnace under an Ar environment at 1273 K for 6 hours before being cooled in the furnace [8]. Thus the heat treatment was done in an Ar atmosphere to avoid the oxidation of the alloys.

2.3 Wear analysis

The wear properties of the alloys were measured using a pin on disc wear testing equipment. Titanium-niobium alloys of various compositions were used to make the pins. The diameter of the pin was 4 mm with a spherical bottom as per ASTM standard G 99-95 A [9]. Three samples of each load were tested using an experimental procedure with dimensions of 20 mm length and 10 mm diameter. The weight loss of the pin is utilized to determine the wear resistance of the alloys.

3. RESULTS AND DISCUSSION

3.1 Initial microstructure

The Microstructure of Ti-Nb alloy is shown at low magnification in Figure 1 (a) and higher magnification in Figure 2 (b). The microstructure consists of microscopic white intermetallic particles and a matrix with a distribution of block-like phases in size range of 8-10 μm. Ti-35Nb-7Zr-5Ta-0.35O consisted of 75±4% and 25±7% phases by volume. Having a lot of Sn in the alloy stabilizes many phases, and it has been claimed that having anywhere from 14 to 34 mass% of Nb in the alloy causes both α and β phases.

The phase in alloy C has a blocky shape (dark region), with sizes ranging from 15-20 μm to 3-5 μm, as shown in Figure 2(a-b). Under a microscope, the matrix's fine intermetallic was evenly dispersed throughout the surface. This alloy had a volume fraction of 62± 4% for the β phase and 38± 7% for the α phase, placing it somewhere in the centre of the other two alloys. Having both stabilizers in the alloy contributes to this effect. Because Nb is a stabilizer, increasing the amount of Nb in an alloy increases the phase proportion. To a similar extent, Sn contributes to the alloy’s creation of

the α phase. As a result, the volume fractions of the two phases lie in the middle, creating this alloy intermediate between the other α phase.

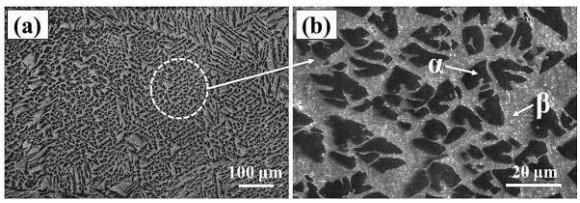


Fig. 1 SEM image of Ti-35Nb-7Zr-5Ta-0.35O (a) Low and (b) High magnification

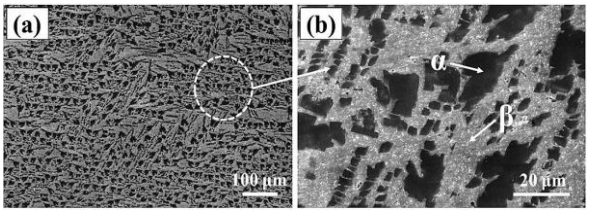


Fig. 2 SEM image of Ti-24Nb-4Zr-8Sn (a) Low and (b) High magnification

3.2 Mechanical Properties

3.2.1 Micro hardness

Table 4.3 displays the results of Vickers microhardness testing on the various phases. The statistics in the table show that the phase is softer than the phase by a factor of almost two (400–470 HV vs 900–1100 HV) (700–750 HV). Adding niobium content significantly increases the hardness of the phase and the phase. Despite the shallow Nb content, this alloy achieves maximum phase hardness thanks to Zr and Sn [11]. When Sn is added to Ti, intermetallics increase the material's hardness. The hardness of the phase was minimal for alloy C due to the low Nb and Sn concentrations. But in the case of alloy B, the hardness of the α phase rose as a result of both increased Nb and the addition of Zr. The ß -phase hardness of the Ti-35Nb-7Zr-5Ta-0.35O alloy was 826±24 HV. This is attributed to the high weight fraction of Nb in the ß phase (~ 41.6 %) together with Sn. The hardness of the ß phase for alloy B was found to be comparatively lower (586 ± 24 HV). This is attributed to the reduced Nb content in the ß phase of the alloy (~ 28.9 %) and the addition of Ta (~ 9.6 %), which results in softening of the ß phase. The low concentration of Nb and Sn in the phase (together accounting for 41.6% of the total weight) is responsible for this. Overall, the phase of alloy Ti-24Nb-4Zr-8Sn was found to have a lower hardness (457±20 HV) than the other phases. It is because the Nb content in the phase of the alloy has been lowered (28.9%), and Ta has been added (9.6%), making the phase softer.

Table 1 Hardness of α and ß phase of the different alloys

Alloy	Hardness (HV)	
	α phase	ß phase
Ti-24Nb-4Zr-8Sn	457±20	735±18
Ti-35Nb-7Zr-5Ta-0.35O	489±14	826±24

3.2.2 Coefficient of friction

For a load of 10 to 30 N, the friction coefficient vs load for all two alloys is plotted in Fig. 3. The Ti-24Nb-4Zr-8Sn alloy's coefficient of friction increased from an initially low value (0.06) to a maximum value (0.52-0.62) across the board when the test loads were increased (10 N, 20 N, and 30 N). For the Ti-35Nb-7Zr-5Ta-0.35O alloy, we saw a similar trend: the coefficient of friction started at 0.08 for light loads and increased to 0.5-0.66 for heavy ones. On the other hand, a Ti-35Nb-7Zr-5Ta-0.35O alloy has a very low coefficient of friction compared to the other two alloys, reaching just 0.37–0.47 for all loads after starting at a value of 0.1–0.2. The frictional properties of the manufactured alloys were comparable to those of common alloys used in biomedical settings (0.5 for Ti-35Nb-7Zr-5Ta-0.35O alloy) [12].

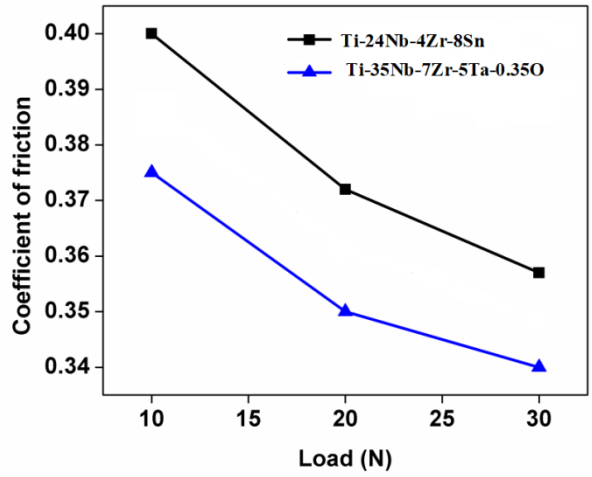


Fig. 3 Coefficient of friction of Niobium alloys

4. CONCLUSIONS

Vacuum arc remelting was successfully fabricated Ti-Nb alloys with compositions including Ti-35Nb-7Zr-5Ta-0.35O and Ti-24Nb-4Zr-8Sn. SEM examined all the cast alloys and found them to be free of flaws like fractures and blow holes.

Compared to Ti-24Nb-4Zr-8Sn alloy, Ti-35Nb-7Zr-5Ta-0.35O exhibited finer ferrite grains.

The Ti-24Nb-4Zr-8Sn alloy has a higher hardness value for the phase (400–470 HV) than for the phase (700–750 HV). Ti-35Nb-7Zr-5Ta-0.35O is a tough alloy because the presence of Ta and Zr considerably increases the hardness of the phase, resulting in a value of 489±14 HV.

The lowest COF is 0.32 μ was obtained for adding Ti-35Nb-7Zr-5Ta-0.35O alloy.

Mechanical characteristics and microstructures of micro-alloyed Ti-35Nb-7Zr-5Ta-0.35O are improved over those of the Ti-24Nb-4Zr-8Sn alloy.

REFERENCES

[1] Yang X, Zhao Z, Bai P, Du W and Wang S (2022) EBSD investigation on the microstructure of Ti48Al2Cr2Nb alloy hot isostatic pressing formed by Selective laser melting (SLM). Mater Letters 309:131334

[2] Dong J, Lin T, Shao H, Wang H, Wang X, Song K and Li Q (2022) Advances in Degradation Behavior of Biomedical Magnesium Alloys: a Review. J Alloys & Comp 164600

[3] Ma Y, Huang Y and Zhang X (2021) Precipitation thermodynamics and kinetics of the second phase of Al–Zn–Mg–Cu–Sc–Zr–Ti aluminum alloy. J Mater Res & Tech 10:445-52

[4] Wanderley KB, Junior AB, Espinosa DC and Tenório JA (2020) Kinetic and thermodynamic study of magnesium obtaining as sulfate monohydrate from nickel laterite leach waste by crystallization. J Cleaner Prod 272:122735
[5] Liu R, Wang W, Chen H, Lu Z, Zhao W and Zhang T (2019) Densification of pure magnesium by spark plasma sintering-discussion of sintering mechanism. Adv Powder Tech 30:2649-58.
[6] Březina M, Hasoňová M, Fintová S, Doležal P, Rednyk A and Wasserbauer J (2021) Mechanical and structural properties of bulk magnesium materials prepared via spark plasma sintering. Mater Today Communic 28:102569
[7] Zhang D, Qi Z, Wei B, Wu Z and Wang Z (2017) Anticorrosive yet conductive Hf/SiC multilayer coatings on AZ91D magnesium alloy by magnetron sputtering. Surface & Coatings Tech 309:12-20
[8] Chen H, Wang J, Meng X, Xie Y, Li Y, Wan L and Huang Y (2021) Ultrafine-grained Mg-Zn-Y-Zr alloy with remarkable improvement in superplasticity. Mater Letters 303:130524
[9] Anand N, Ramachandran KK and Bijulal D (2021) Microstructural, mechanical and tribological characterization of vacuum stir cast Mg-4Zn/SiC magnesium matrix nanocomposite. Mater Today: Proceed 46:9387-91
[10] Naghizadeh A, Ekolu SO and Musonda I (2020) High temperature heat-treatment (HTHT) for partial mitigation of alkali attack in hardened fly ash geopolymer binders. Case Studies in Construct Mater 12: e00341
[11] Zhao Z, Zhao R, Bai P, Du W, Guan R, Tie D, Naik N, Huang M and Guo Z (2022) AZ91 alloy nanocomposites reinforced with Mg-coated graphene: Phases distribution, interfacial microstructure, and property analysis. J Alloys & Comp 902:163484
[12] Zhao J, You C, Chen M, Lyu S, Tie D and Liu H (2021) Effect of calcium oxide particle size on microstructure and properties of AZ91 Mg alloy. J Alloys & Comp 886:160970.